 DOI: 10.1002/masy.200650906

An AFM Study of Poly(L-lactic acid) and Poly(D-lactic acid) Macromolecules and Their Stereocomplexes at the Solid-Air Interface

Ashok Narladkar, Eric Balnois, Yves Grohens*

Summary: The self assembly of PLA enantiomers have been studied at the nanometer scale using atomic force microscopy. At first, the conformation of D and L PLA macromolecules in dilute regime and the initial state of aggregation of both enantiomers were successively observed and compared with the aggregation of PLLA/PDLA blends. Our results points out differences in the aggregates structure between the homo-aggregates of each enantiomers and the 3 Dimensional stereocomplexes formed with racemic mixture of D and L entities. On the one hand, D or L PLA chains, which adopt a rigid conformation in dilute regime, form gradually aggregates that tend to grow from a nucleation center. On the other hand, stereocomplexes have a non-compact structure and are elongated with height variations within the fibrils that support the side by side aggregation of D and L helical structures to form thicker fibrils.

Keywords: AFM; aggregation; PLA; stereocomplexation

Introduction

Poly(lactide) (PLA) is among the most important biopolymer used in various applications, including medical devices such as drug delivery systems, surgical sutures and implants, [1,2] their use as matrix materials in bioresorbable composites [3] due to its biocompatibility and biodegrability. These two interesting characteristics make it also a promising candidate for bioplastic bag and films applications. This biopolymer can be produced from renewable resources such as cornstarch or sugar beet and high molar weight PLA macromolecules can be produced by ring-opening polymerization of cyclic lactides monomer in the presence of catalyst [4,5]. It degrades to non-toxic latic acid, which is naturally present in the human body. Another original characteristic of this biopolymer is its ability to form stereocomplexes between its two opposite enantiomeric configurations, the L and D PLA forms. The so-formed stereocomplexes show different physicochemical behaviour compared to their parent polymers but are still biocompatible. An important characteristic of PLA stereocomplexes is for example an increase in its melting temperature transition ($\sim$+50 °C) in comparison to the melting temperature of the crystal of the pure PLA enantiomers [6]. It was also reported in the literature that the stereocomplex crystal, formed by packing B form 3_1 helices of opposite configuration side by side, exhibits a lamellar and triangular type morphology, as revealed by atomic force microscopy (AFM) in comparison with the lozenge shaped crystals well known for pure enantiomeric PLA crystal [7,8]. Another important change in properties of the stereocomplex is its insolubility in common solvents. The stereocomplex was for example found to be insoluble in chloroform [9]. Other studies deal with the investigation of parameters such as the D/L ratio on the thermal property and crystallisation behaviour of the PDLA/PLLA blends [10].

Laboratoire Polymères, Propriétés aux Interfaces et Composites (L2PIC), Université de Bretagne Sud, BP 92116, 56321 Lorient Cedex, France

It clearly appeared from the literature that numerous studies have been performed on the study of the properties of the stereocomplexes and mainly on their crystalline structure. The above characteristics are intimely linked to the intrinsic characteristic of polymer individual chains. Surprisingly, only few papers described the characteristics of PLA macromolecules [11–13]. For example, Cornelis *et al.* [11] measured using light scattering a greater chain stiffness for PLLA (with a characteristic ratio C_∞ of 11.8) compared to racemic D, L PLA (with C_∞ of 9.5). This difference in chain stiffness is claimed to be the governing factor for the glass transition temperature of poly (D,L-lactide) (*i.e.* the higher T_g at higher L lactide contents could be explained by an intrinsically greater chain stiffness). More recently, Kang *et al.* [13] used static and dynamic light scattering techniques, in addition with Raman spectroscopy, to estimate the characteristic ratio C_∞, and confirm the inherent rigidity of the PLLA chains (with a characteristic ratio C_∞ of 12.4) that decreases as the regio-regularity decreases. Furthermore, their dynamic light scattering studies also demonstrate the rigidity of the PLLA chains by measuring a $\langle R_g \rangle / \langle R_h \rangle$ ratio of 2.57, typical of a rod-like conformation, that decreases as a function of D content within the D,L PLA polymer. In another recent study, Anderson and Hillmyer [14] used small angle neutron scattering to determine the statistical segment length of different PLA samples and also observed that the chain dimensions were decreasing with increasing temperature and increasing D content.

These studies clearly demonstrate that the PLLA homopolymer is highly rigid and that this rigidity decreases upon mixing the D and L enantiomers. Nonetheless, no consensus is still found on the molecular mechanism of cross-linking in stereocomplexation that tends to decrease the polymer chain rigidity as previously described. The objective of this work is therefore to gain an understanding in the conformation of PLLA and PDLA enantiomers and on the initial stage of stereocomplexation, using the atomic force microscopy (AFM).

Experimental Section

Materials

The polymers Poly (L-lactic acid) and Poly (D-lactic acid) were kindly provided by PURAC Biochem BV (Gorinchem, The Netherlands). The viscosimetric molar weight (M_v) of PLLA and PDLA, measured from viscosity measurements, were found to be 99 000 g mol^{-1} and 100 000 g mol^{-1} respectively.

Sample Preparation

PDLA and PLLA samples were dissolved in methylene dichloride (CH_2Cl_2) to a final concentration of 1000 g L^{-1}. The solution was gently stirred during 24 hours at room temperature to ensure a complete dissolution of the polymer. From this stock solution, different diluted solutions were prepared at concentrations of 1000 mg L^{-1}, 100 mg L^{-1} and 10 mg L^{-1}. PLA stereocomplexes were prepared using the method described elsewhere [9]. Briefly, PDLA and PLLA solutions, at same concentrations of 1000 mg L^{-1}, 100 mg L^{-1} or 10 mg L^{-1} respectively, were mixed together in a 1:1 ratio and the resulting solution was gently stirred during 30 minutes.

Atomic Force Microscopy (AFM)

PLA solutions were deposited onto freshly cleaved mica using the drop deposition method. In the drop deposition method, 5 μL of solution was simply deposited on freshly cleaved mica. The samples were then allowed to evaporate under ambient conditions (25 °C and 55% of relative humidity) in a Petri Dish during at least 20 min before the AFM observation.

AFM images were obtained under ambient conditions (23 °C and 60% of relative humidity) using light tapping mode AFM (TM-AFM) on a multimode scanning probe microscope (Nanoscope IIIa, Veeco). The ratio of the setpoint amplitude to the free amplitude was maintained approximatively at 0.9. RTESP AFM tips (Veeco), with

typical resonance frequency between 300 and 400 KHz and with tip radius between 5–15 nm were used. Height and length measurements of the deposited macromolecules were made using the section analysis software of the microscope (V6.13r1 by Digital instruments).

For each sample, at least five replicate samples were prepared and on each sample, a minimum of five different areas on the surface were investigated to ensure a good reproducibility of the AFM observations.

Results and Discussion

Throughout this section, PLA species are classified as: (i) isolated molecular species (simple helices of PLA), (ii) aggregates (formed by the association of at least two individual PLA helices) or (iii) gel-like structures (formed by a network of interconnected macromolecules).

Effect of the Enantiomeric Composition of the PLA

Figures 1A and 1B are examples of a TM-AFM image of PLLA and PDLA respectively deposited on mica from 10 mg L^{-1} solutions using the drop deposition method.

Both images demonstrated the coexistence of homogeneously dispersed aggregates and some isolated macromolecules of PLA on the mica surface, these latter adopting a fairly elongated shape, characteristic of a fairly rigid polymer structure. This observation is in good agreement with the helical structure that is usually reported for PLA macromolecules. The rod like large aggregates, are entities formed by the association of several individual chains. These aggregates are not present in solution but could be due to the sample preparation method, including a drying step, which induces gradients of concentration, possibly phase separation and therefore leads to inter-chain associations. Nonetheless, it is worth mentioning that the proportion of aggregates versus isolated macromolecules varies according to the enantiomer, with a larger proportion of aggregates observed for the PLLA sample (Figure 1A) whereas only few of them could be seen for the PDLA sample. This demonstrates that, even if the chemical composition of the two enantiomers is the same, their behaviour at interfaces (conformation) is slightly different.

It has to be pointed out that the observed structures of PLA on mica may not be necessarily representative of their structure in solution, as already reported for other AFM studies on different polymers [*e.g.* 15,16]. If on the one hand, DNA molecules were found to adopted an equilibrated 2D conformation on mica, with measured L_p values from AFM images in agreement with persistence length (L_p) values of DNA in solution [15], on the other hand, succinoglycan macromolecules, an anionic polysaccharide, were found to adopt a non equilibrated configuration when deposited from a water and low ionic strength solutions on mica surface [16]: the measured end to end distance of the macromolecules was found to be similar to a projected 3D end-to-end distance, rather than a 2D equilibrated one. Consequently, the measured persistence length of the macromolecules, from the AFM images, was higher than the one obtained from light scattering measurements, in good correlation with the fact that succinoglycan macromolecules are likely to adopt a more extended conformation than that occurring in solution due to a charge repulsion with the negatively charged mica. The systematic effect of the surface and the deposition conditions on the conformation of PLA is under investigation and was, to the best of our knowledge, not reported in the literature.

Nonetheless, it is worth mentioning that the proportion of aggregates versus isolated macromolecules varies according to the enantiomer, with a larger proportion of aggregates observed for the PLLA sample (Figure 1A) whereas only few of them could be seen for the PDLA sample. This demonstrates that, even if the chemical composition of the two enantiomers is the same, their behaviour at interfaces (conformation) is slightly different.

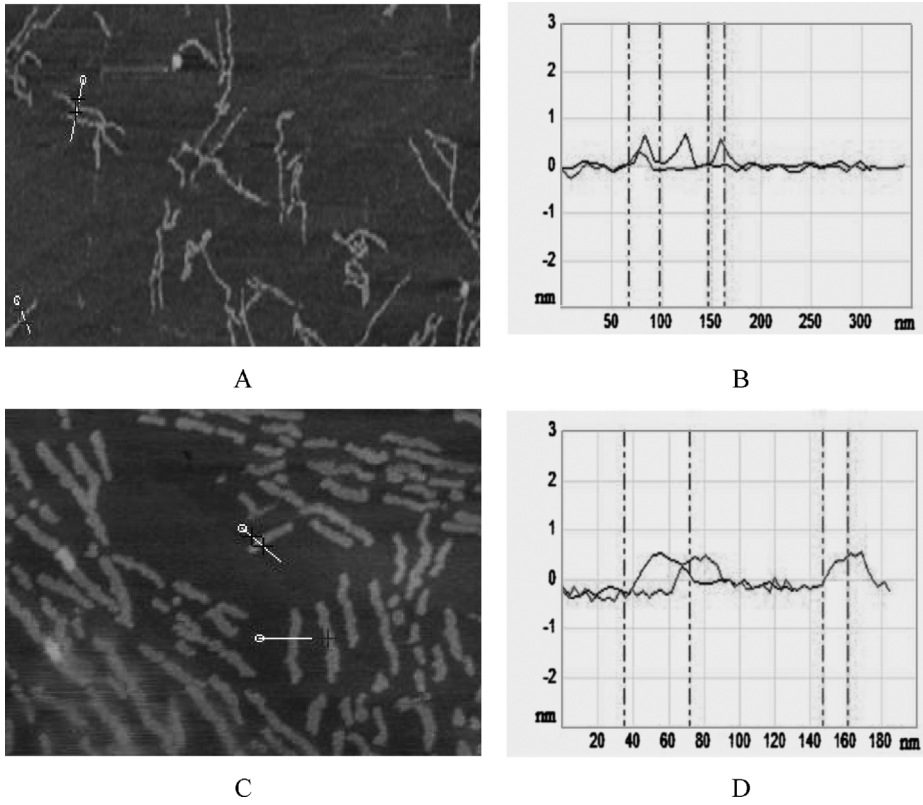

Figure 1.
Tapping mode AFM images (images scan size is 2.5 μm × 2.5 μm) of A): PLLA macromolecules deposited on mica using the drop deposition method; B) corresponding cross section analysis showing the height of the polymer chains; C) PDLA deposited on mica using the same deposition technique; D) corresponding cross section analysis.

Figures 2A represents the height distribution of PLLA and PDLA individual macromolecules respectively. In both cases, the height of the chains was found to be between 0.4 and 0.7 nm. These values are consistent with the crystallographic b value of 0,598 nm obtained for polymer single crystals by electron diffraction methods [7]. Figure 2B shows the end-to end distances histograms of both macromolecules and reveals that PLLA chains adopted more elongated structures on mica ($\langle R_{ee}\rangle_{PDLA} = 255 \pm 35$ nm and $\langle R_{ee}\rangle_{PLLA} = 267 \pm 36$ nm). The result obtained on the PLLA sample has to be interpreted cautiously since for this sample, individual macromolecules are difficult to identify and the reported value may integrate a large number of aggregates. Nevertheless, the contour length of a fully extended PLA chain state of 100 000 $g \cdot mol^{-1}$ in a trans-trans configuration is 1500 nm, which is far larger than the values measured here. According the C_∞ of 12, the end-to-end distance of PLA in solution is about 35 nm. The larger value of 200 to 300 nm is ascribed to stretched helix in a 3_1 conformation which could yield this range of value.

Effect of the Concentration

Figure 3 and 4 represent typical images obtained from the deposition of more concentrated D and L PLA solution of 100 mg L^{-1} and 1000 mg L^{-1} respectively on mica. The well known aggregating effect of the drop deposition method is pointed

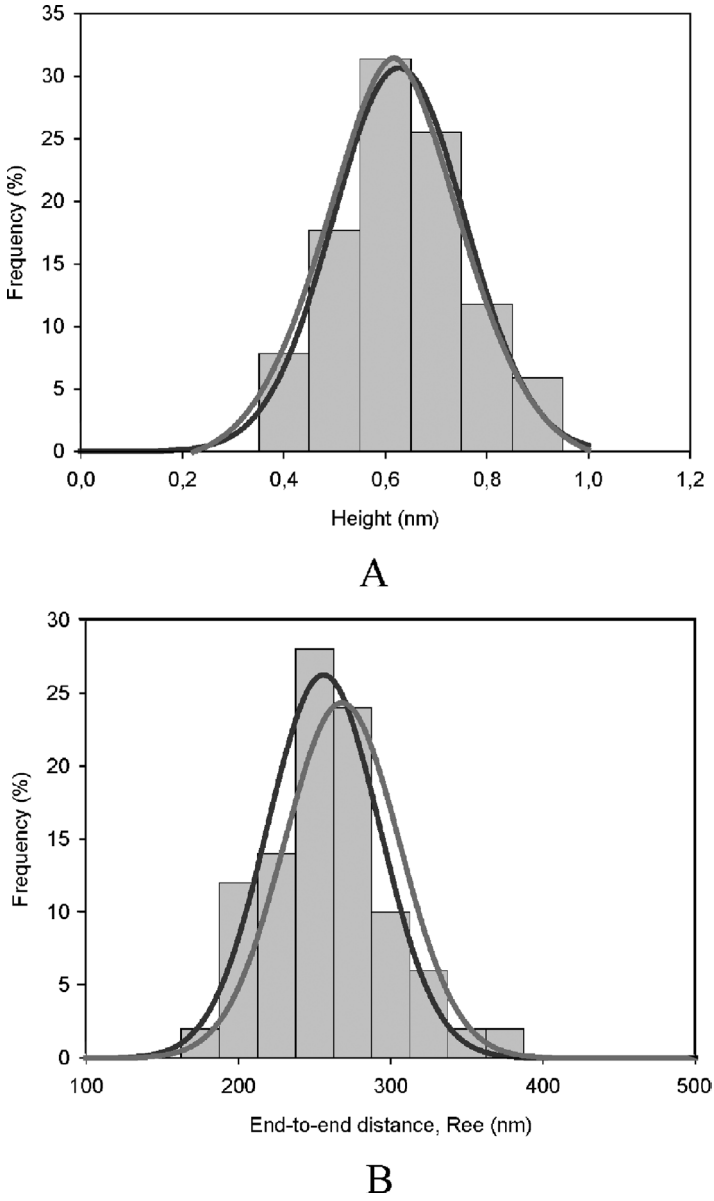

Figure 2.
Histograms of A) height of PLLA (red line) and PDLA (blue line) samples and B) end-to-end distances for the PLLA (red line) and PDLA (blue line) samples.

out in these experiments since the concentration of aggregates increases on the mica surface. The interesting observation is the observation of the initial stage of aggregation of PLA enantiomers on mica and the study of the effect of the initial configuration of the individual chains on the resulting aggregated structure. In both images, large fibrilar aggregated structures tend to grow from a central point with spherical shape, such as micelle-like structures. The center of the micelle seems to act as a nucleation point from which the polymer superstructures start to associate and spread on the surface.

A zoom on these structures (Figures 3B and 3D) allows to reach a better resolution

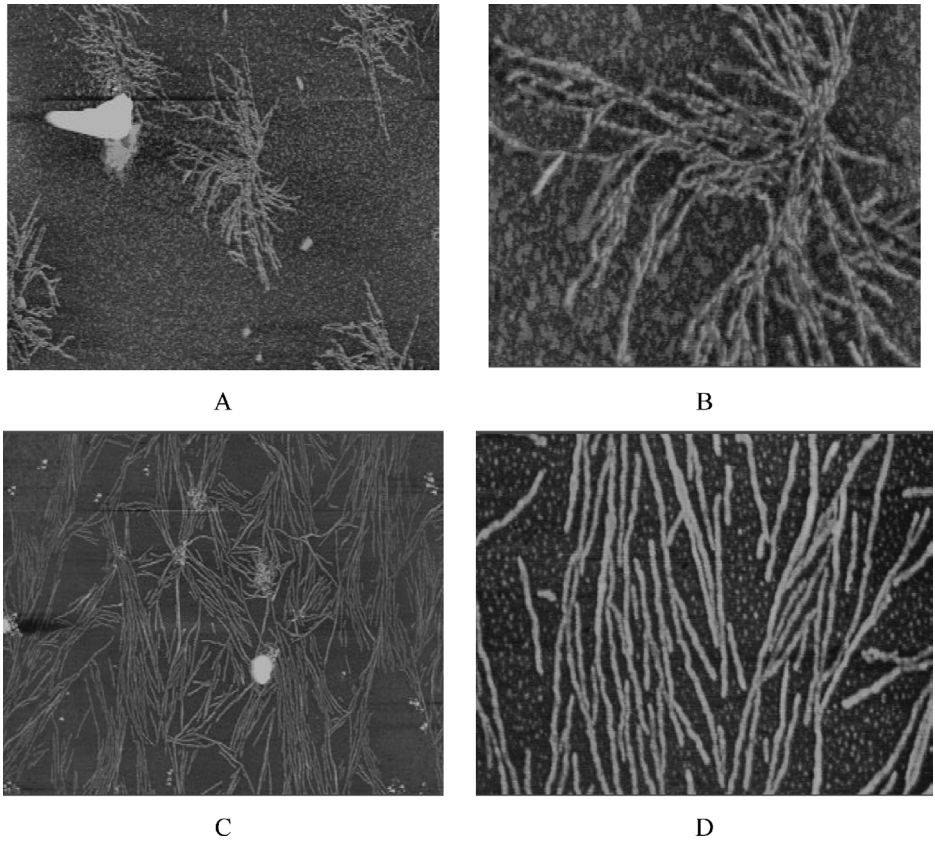

Figure 3.
Typical AFM images of (A) PLLA deposited on mica from a 100 mg · L^{-1} solution (scan size is 10 μm × 10 μm); (B) Zoom of the same sample showing the center of nucleation of the aggregate (scan size is 2.5 μm × 2.5 μm); C) PDLA deposited on mica from a 500 mg L^{-1} solution (scan size is 10 μm × 10 μm); D) zoom of the same sample showing that the associated molecules are formed by the connection of the rigid individual macromolecules (scan size is 2.5 μm × 2.5 μm).

on the internal aggregate structure. For the PLLA aggregate, the macromolecular chains appear to be more or less intertwisted whereas for the PDLA structure, the aggregate is constituted with the individual rigid and linear macromolecules which seem to be well separated within the structure. This observation may generate various stereocomplex structures by directly forming the stereocomplex from initially deposited macromolecules as already mentioned by Serisawa *et al.* [17].

When the concentration is further increased to 1 g L^{-1} (Figure 4), the structuration of both enantiomers is still controlled by the initial conformation of the macromolecules. The AFM image of the PLLA sample reveals that, at this concentration the mica surface is covered by a nearly completed film of PLA.

Cross sections reveal that the heights of the fibrils forming the film are within the size of the initially formed aggregates or isolated entities, *i.e.* 0.6–0.9 nm. At this concentration, the PLA macromolecules and aggregates are interconnected and almost cover the mica surface. The particular orientation of the fibrils within the film is probably generated by the initial ''micellar'' structuration that takes place at

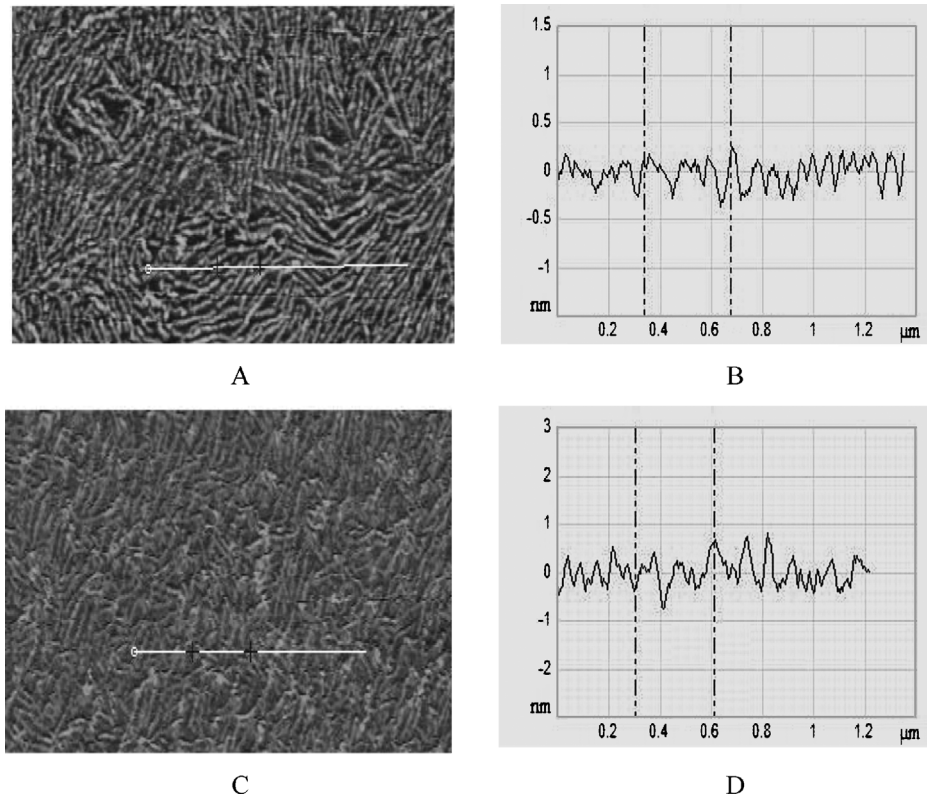

Figure 4.
Typical AFM images (2.5 μm × 2.5 μm) of PLA solutions at 1 g L^{-1} deposited on mica using the drop deposition method: (A) PLLA solution; (B) corresponding cross section analysis; (C) PDLA solution; (D) corresponding cross section analysis.

1 g L^{-1}. This effect is less evident for the PDLA samples which seem to adopt a more compact film structure. This difference can be explained by the more linear structure of individual PDLA macromolecules at lower concentration (mainly isolated chains in contrast with PLLA aggregates) which could allow a more compact organisation of the chains in the film at higher concentration.

For a concentration of the deposited solution of 10 g L^{-1}, a homogeneous and smooth film is formed on the mica surface following the evaporation of the solvent (Figure 5). The film is 3 to 4 nm thick and its roughness (RMS value) is about 0.4 nm. Some spherical holes can also be observed within the film. These holes may be due to the drying effect. Similar structures were already reported in the literature for PI-PLA or PS-PLA block copolymers in the literature [e.g. 18]. Furthermore, Amgoune *et al.* [18] demonstrate that the PI-PLA film structure was dependent on the stereoregularity of the PLA block copolymer and consequently, that the structure of the block, either isotactic or heterotactic, was influencing the morphology of the film.

For the two enantiomers, a film with few spherical holes can be observed. If the roughness of the films is similar, their height and the holes diameter were found to be higher for the PDLA samples (4 nm and 200 nm in comparison with 2 nm and 100 nm for the PLLA). These differences may certainly result from the initial differ-

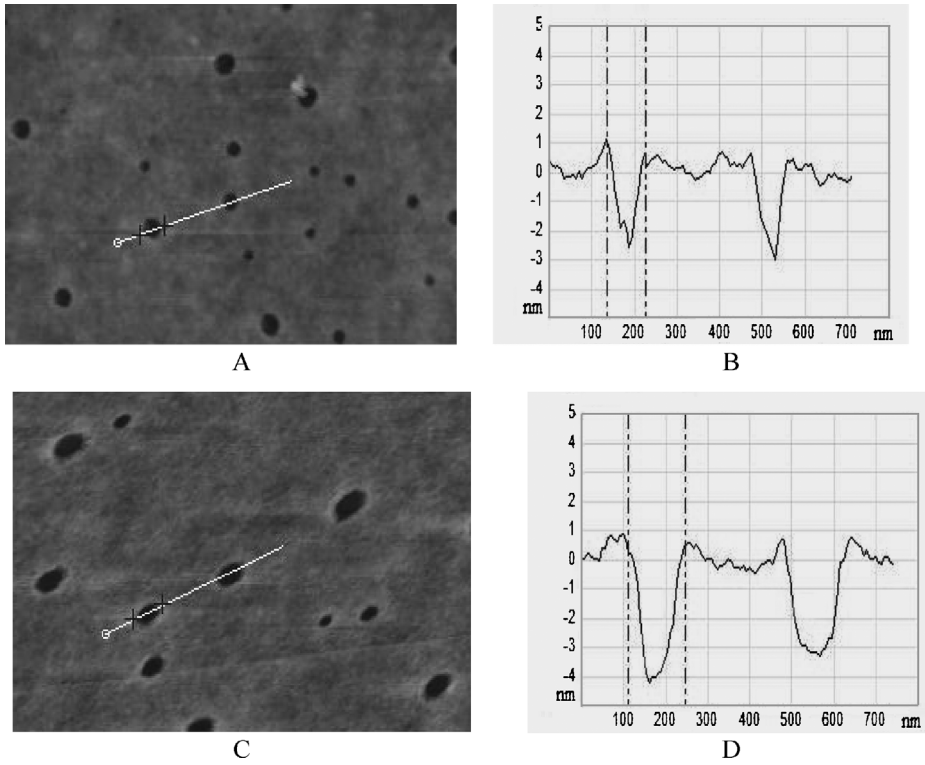

Figure 5.
AFM images (2.5 μm × 2.5 μm) of PLA solutions at 10 g L^{-1} deposited on mica: A) PLLA solution; B) corresponding cross section analysis; C) PDLA solution; D) corresponding cross section analysis.

ent conformation of the two enantiomers and the resulting structuration of the aggregates when the concentration is increased.

Stereocomplexation of PLLA and PDLA

The stereocomplexation between the D and L PLA enantiomers has been studied using the same strategy. At first, the stereocomplexes were formed in solution and then deposited on a mica surface, according to solution concentrations, from 100 mg L^{-1} up to 10 g L^{-1}. Figure 6 reports typical AFM images obtained when the solution concentrations are 10 mg L^{-1}, 1 g $L^{-1}$and 10 g L^{-1} respectively.

The D,L-PLA stereocomplex structure, as revealed in figure 1, contrasts with the structure formed by the two enantiomers at the same solution concentration (Figure 1A and 1C). Only few aggregates can be found on mica, indicating an important interaction between both enantiomers. The aggregate looks like interconnected fairly elongated and rigid fibrils such as a network structure. The height of the fibrillar chains within the stereocomplex was found to be *i)* higher than isolated PLLA and PDLA macromolecules, suggesting that the fibrils are already aggregates of PLA, consisting at least of two or several chains and *ii)* varying within the stereocomplex network (from 0.6 up to 2 nm), suggesting some degree of side by side aggregation of helices. The branching character of the aggregates and the fairly opened structure, in comparison with the homoaggregates (D or L), also support the idea that the association within the D and L PLA entities is kinetically driven. These results can be

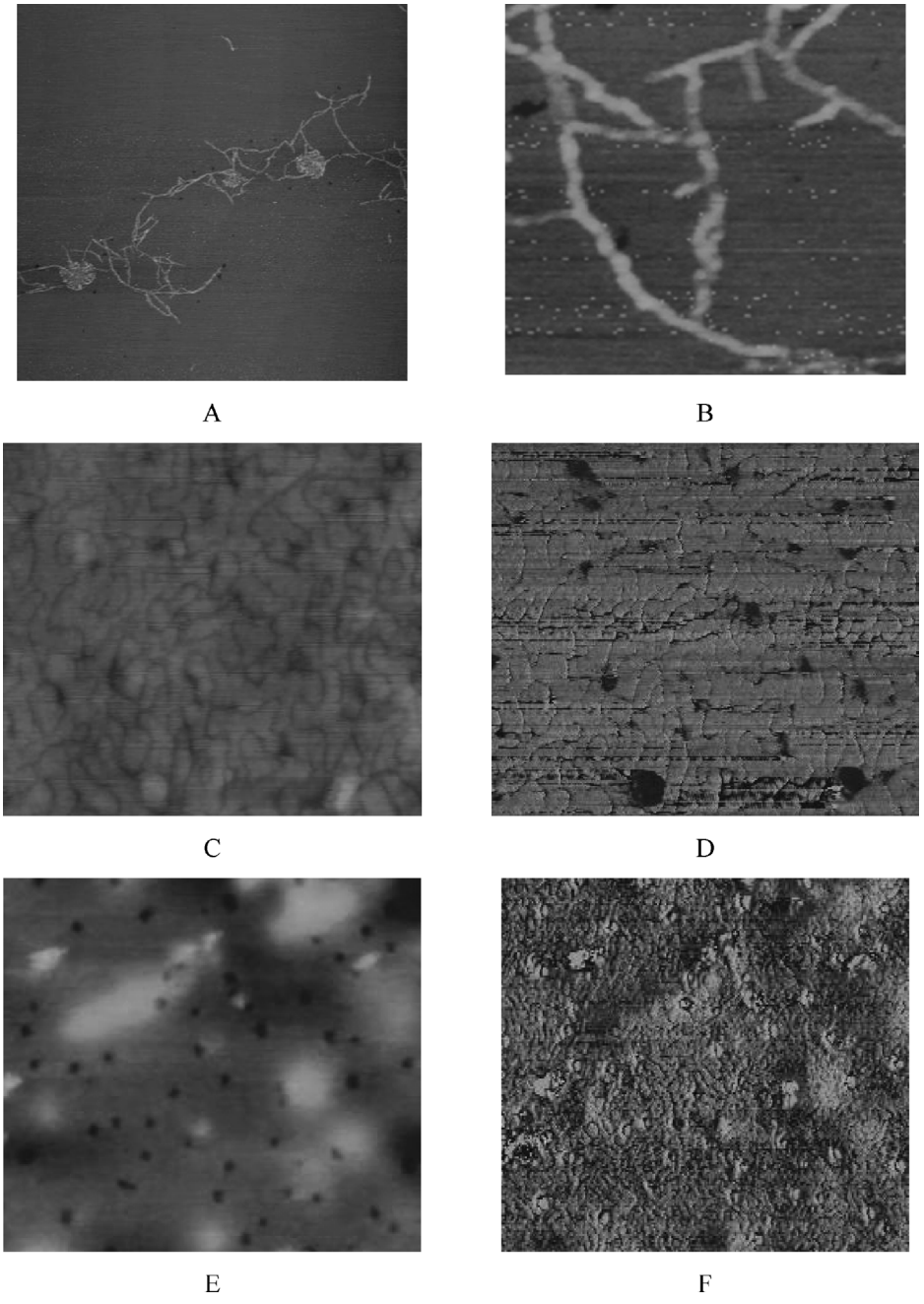

Figure 6.
Stereocomplex of racemic (D,L) PLA solutions as a function of concentration. A) AFM height image (5 μm × 5 μm) of a typical stereocomplex structure obtained for a solution of 100 mg L^{-1}; B) Zoom on the stereocomplex structure showing the well ordered fibrils (600 nm × 600 nm); C) AFM height image (2.5 μm × 2.5 μm) and, D) corresponding phase AFM of stereocomplex structures observed on mica at 1 g L^{-1}; E) AFM height image (5 μm × 5 μm) and, F) corresponding phase AFM of stereocomplex structures observed on mica at 10 g L^{-1}.

correlated with the work of Klass *et al.* [19] who studied the surface pressure-area (π-A) isotherms of enantiomeric PLA and their stereocomplex at the air-water interface using Polarization Modulated Infra-Red Reflection-Absorption Spectroscopy (PM-IRRAS). The authors observed similar (π-A) isotherms at the air-water interface for poly(L-lactide) and poly(D-lactide) but a different one for the D-L blend. Their measurements established that the conformation of the helical PLA chains and the D/L blend at the air-water interface was different. Furthermore, they state that the PLA and D/L blend monolayer differ in their kinetics, suggestive of difference in packing state.

Based on qualitative observation from AFM images, it seems that D/L blends aggregates present inhomogeneities proved by their difference in heights. Such inhomogeneity is not observed for the pure PDLA or PLLA samples, since native helical structures could form superstructures that are probably homogeneously packed helices. In the case of the D,L blend, the difference in conformation between the D and L macromolecules may generate association of helices from partial part of the chains into network junction.

At a concentration of 1 g L^{-1}, the AFM images reveal the presence of aggregated structures which are homogeneously distributed on the surface. The structures are different from the two homopolymers aggregates and therefore suggest that they are heteroaggregates.

Finally, at concentration of 10 g L^{-1}, a homogeneous film, with some holes, covering the mica surface is observed. Nonetheless, if the film height and the holes diameters (around 100–200 nm) were equivalent to those obtained for both enantiomeric films, its roughness was found to be higher (RMS about 2.5 nm) as confirmed by the phase image contrast. This latter image allows to distinguish fibrils interconnected fibrils within the film. The observed phase contrasted structures are similar to those formed at 1 g L^{-1}.

When stereocomplexation is allowed to proceed in methylene dichloride solution, heteroaggregation between D and L PLA macromolecules occur and give rise to a three dimensional structures that are morphologically different from the homoaggregates obtained for both PLA enantiomers. The long and interconnected structure of the aggregates may be due to the formation of stereocomplex microcrystallites which act as cross-links. Occurence of 3D gelation at low concentrations indicates that stereocomplex crystallites simultaneously form under existence of a high density of PLLA and PDLA chains. Its elongated, higher and branched structure suggests some degree of side by side aggregation between helices, leading to multiple associations of helices rather than association by multiple helices.

Conclusion

AFM has been shown to be a versatile tool for investigating the conformation of PLA enantiomers and their aggregation mechanisms. Our results give a direct visualisation of the rigid helical structures of both D and L PLA chains and demonstrate a different mechanism between aggregation of each enantiomers and the 3 Dimensional stereocomplexation of racemic mixture of D and L entities. The resulting stereocomplex structure is a non-compact and fairly elongated fibrillar network with few branches. Moreover, the diameter of the fibrils within the aggregates is found to be higher than the diameter of the enantiomeric macromolecules and/or aggregates. Our result supports the side by side aggregation of D and L helical structures into thicker branches. Furthermore, the non compact structure also suggests the importance of the kinetic of formation of the stereocomplex.

Acknowledgements: We thank PURAC Biochem BV (Gorinchem, The Netherlands), for kindly supplying the PLA samples.

[1] A.J. Domb, N. Kumar, T. Sheskin, A. Bentolila, J. Slager, T. Teomim, '' *Polymeric biomaterials*'', Marcel Dekker, New York 2001.
[2] A. Slager, A.J. Domb, *Adv. Drug Del. Rev.* **2003**, *55*, 549.
[3] K.R. St. John, '' *Biocompatible Polymers, Metals, and Composites*'', Technomic Publishing Co.: Lancaster, PA, 1983.
[4] E. Lillie, R.C. Schultz, *Makromol Chem* **1975**, 176, 1901;
[5] F.E. Kohn, J.W.A Van den Berg, G. Van de Ridder, J. Feijen, *J. Appli. Polym. Sci.* **1984**, 29, 4265.
[6] H. Tsuji, S.H. Hyon, Y. Ikada, *Macromolecules* **1992**, 25(11), 2940.
[7] D. Brizzolara, H.-J. Cantow, K. Diederichs, E. Keller, A.J. Domb, *Macromolecules* **1996**, *29*, 191.
[8] Y. Ikada, K. Jamshidi, H. Tsuji, S.H. Hyon, *Macromolecules* **1987**, 20, 904–906
[9] H. Tsuji, S.H. Hyon, Y. Ikada, *Macromolecules*, 1991, 24, 5657.
[10] H. Yamane, K Sasai, *Polymer* **2003**, 44, 2569.
[11] A. Cornelis, C.A.P. Joziasse, H. Veenstra, D.W. Grijpma, A.J. Pennings, *Macromol. Chem. Phys.* **1996**, 197, 2219.
[12] D.W. Gripjma, J.P. Penning, A.J. Pennings, *Colloid. Polym. Sci.* **1994**, 272, 1068.
[13] S. Kang, G. Zhang, K. Aou, S.L. Hsu, H.D. Stidham, X. Yang, *J. Chem. Phys.* **2003**, 118, 3430.
[14] K.S. Anderson, M.A. Hillmyer, *Macromolecules* **2004**, 37, 1857.
[15] C. Rivetti, M. Guthold, C. Bustamante, *J. Mol. Biol.* **1996**, 264, 919.
[16] E. Balnois, S. Stoll, K.J. Wilkinson, J. Buffle, M. Rinaudo, M. Milas, *Macromolecules* **2000**, 33, 7440.
[17] T. Serizawa, H. Yamashita, T. Fujiwara, Y. Kimura, M. Akashi, *Macromolecules*, **2001**, 34(6), 1996.
[18] A. Amgoune, C.M. Thomas, E. Balnois, Y. Grohens, P.J. Lutz, J.-F. Carpentier, *Macromol. Rapid Commun.* **2005**, 26, 1145.
[19] A. Klass, R.B. Lennox, G.R. Brown, H. Bourque, M. Pezolet, *Langmuir* **2003**, 19, 333.

